

Regime shifts in marine ecosystems of the North Sea and Wadden Sea

Mariska Weijerman¹, Han Lindeboom^{1,*}, Alain F. Zuur²

¹Royal Netherlands Institute for Sea Research, PO Box 597, 1790 AD Den Burg, Texel, The Netherlands

²Highland Statistics Ltd., 6 Laverock Road, Newburgh AB41 6FN, Aberdeenshire, UK

*Corresponding author. Email: han.lindeboom@wur.nl

Marine Ecology Progress Series 298:21–39 (2005)

Appendix 1. Overview of publications on long-term variation in marine ecosystems of NW European shelf. ICES: International Council for Exploration of the Sea; NAO: North Atlantic Oscillation

Regulatory variables	Response variables	Location	Time period	Source
Hydrography	Temperature and salinity	ICES area	1980–1990	Ellett & Blindheim (1992)
Wind stress, turbulence effects, cloud coverage water	Biological productivity	Northern and central North Sea	1968–1990	Svendson & Magnusson (1992)
Wind	Temperature and salinity	Southern North Sea and Barents Sea	1970–1989	Furnes (1992b)
Wind	Transport fluxes	Norwegian trench	1881–1989	Furnes (1992a)
Wind	Wave	North Atlantic	1968–1993	Gulev & Hasse (1999)
NAO	Water inflow	Nordic waters	1955–1996	Mork & Blindheim (2000)
Wind forcing	Wind speed	North Sea	1958–1997	Siegismund & Schrum (2001) ^a
Tidal motion, wind	Temperature, salinity, sea level	North Sea	Review	Otto et al. (1990)
Mean sea level rise	Accretion of salt marshes	Wadden Sea	1968–1992	Dijkema (1997) ^a
River water input, eutrophication	Phytoplankton biomass and diversity	German Bight	1980–1990	Hickel et al. (1992)
Physical parameters, Atlantic inflow	Zooplankton diversity	North Sea along eastern UK coast	1958–1995	Lindley & Batten (2002)
Benthos	Mesozooplankton diversity	Central North Sea	1958–1994	Lindley et al. (1995)
Air stream, fresh surface-water inflow	Dinoflagellate abundance	North-central North Sea	1958–1990	Dickson et al. (1991)
Temperature, NAO	<i>Calanus finmarchicus</i> and <i>C. helgolandicus</i> abundance	Northern North Sea	1958–1996	Beare & McKenzie (1999)
Eutrophication	Benthic communities and phytoplankton biomass	Western and eastern North Sea	1973–1988	Austen et al. (1991)
Eutrophication	Phytoplankton primary production, chlorophyll <i>a</i> , organic carbon fluxes and turbidity	Marsdiep	1974–1990	Cadée & Hegeman (1991b)
Eutrophication	<i>Phaeocystis</i> sp. blooms	Marsdiep	1965–1989	Cadée & Hegeman (1991a)
Eutrophication	Phytoplankton biomass, primary production and <i>Phaeocystis</i> sp. blooms	Marsdiep	1974–2000	Cadée & Hegeman (2002) ^a

Appendix 1 (continued)

Regulatory variables	Response variables	Location	Time period	Source
NAO (temperature)	Phytoplankton biomass	NE Atlantic and North Sea	1960–1995	Edwards et al. (2001)
North Atlantic current dynamics, NAO	Plankton communities	North Sea	1960–1995	Edwards et al. (2002)
Eastern shelf edge current	Plankton communities	North Sea	1948–2000	Reid et al. (2001b)
Physical parameters, Atlantic inflow	Neritic zooplankton	North Sea	1958–1998	Beare et al. (2002)
Physical and chemical factors	Phytoplankton blooms	ICES area	Review	Colijn (1991)
NAO	Phytoplankton colour index	Central North Sea, Atlantic	1948–1995	Reid et al. (1998)
NAO (temperature)	Calanoid copepod distribution	Eastern North Atlantic, European Shelf seas	1960–1999	Beaugrand et al. (2002)
NAO (temperature)	Macrofauna communities	German Wadden Sea (off Norderney)	1978–1995	Kröncke et al. (1998)
Eutrophication	<i>Temora longicornis</i>	Marsdiep	1973–1991	Fransz et al. (1992)
Pelagic phytoplankton biomass	Macrozoobenthic biomass	Marsdiep, Balgzand	1974–1995	Beukema et al. (2002) ^a
Winter temperature	Macrobenthos dynamics	Balgzand	1969–1988	Beukema (1990)
Winter temperature	Macrobenthic predator prey relation	Wadden Sea	1970–1997	Beukema et al. (2000)
Winter temperature, eutrophication, oxygen deficiency	<i>Phoronis mülleri</i> abundance	SE North Sea (German Bight)	1964–1988	Nierman (1996)
NAO	Macrofauna invertebrates in streams and rivers	Rivers in central Wales	1986–2000	Bradley & Ormerod (2001)
Sedimentation of pelagic production	Benthic community structure	North Sea	1970–1990	Josefson et al. (1993)
Fishing	Macrobenthic fauna, abundance and composition	NE coast of England	1971–1998	Frid et al. (1999)
Local and mesoscale physical factors	<i>Abra alba</i> community	NW coast of France	1978–1992	Fromentin et al. (1997)
Eutrophication, anthropogenic pollution, hydrologic conditions, overfishing	Fish community	NE slope of Gulf of Riga	1974–1996	OJaveer (1996)
Fishing mortality	Cod stock size and recruitment	North Sea	1960–1990	Daan et al. (1994)
May temperature	Squid <i>Loligo forbesi</i> abundance	Around Scotland	1970–1996	Pierce & Boyle (2003)
NAO	Herring fishery	Swedish coast of Bohuslän	1895–1978	Alheit & Hagen (1996)
NAO	Horse mackerel fishery	North Sea	1976–1994	Reid et al. (2001a) ^a
Environmental factors	Fish recruit abundance	Marsdiep	1972–1994	Philippart et al. (1996) ^a
Temperature	Plaice recruitment	North Sea		Fox et al. (2000)
Climate variability	Fish community (trophic-level fisheries)	Celtic Sea	1948–2002	Pinnegar et al. (2002)
Bottom temperature	Timing of squid migration	SW England	1953–1972	Sims et al. (2001)
Temperature	Whiting abundance	Northern North Sea		Zheng et al. (2002)
Temperature, solar cycle	Marine organisms (survival, reproductive success, dispersal patterns)	Western English Channel	1924–1988	Southward et al. (1995)
NAO	Aquatic and marine ecosystems	North Atlantic region	Review	Ottersen et al. (2001)
	Number of eider fledglings	Wadden Sea, Vlieland	1962–1988	Swennen (1991) ^a

^aData used in this study

Appendix 2. Long-term data series used in this study: sources, and pattern over time

A total of 78 data series were analysed: 28 environmental data sets comprising atmospheric, solar, climate and oceanographic variables; and 50 biological time series representing a wide range of marine organisms including marshland vegetation, micro- and macro-flora and fauna, fish species, bird species and mammals. Detailed information for each time series is given below in the following format: the series code used in the paper, followed by the series name, e.g. NAOWIN: North Atlantic Oscillation winter index (December to March average). For each series, we then include our source for the data, a short descriptive paragraph, and a figure (at the end of the Appendix) showing the pattern of the time series standardized to zero mean and unit standard deviation. The presumed regime shifts (1978 or 1979 and 1988 or 1989) are indicated by vertical bars in each figure.

Atmospheric indices

NAOWIN: North Atlantic Oscillation winter index (December to March average)

Source: www.met.rdg.ac.uk/cag/NAO/index/html

One of the most prominent teleconnection patterns in all seasons is the North Atlantic Oscillation (NAO). The NAO index represents the pressure difference between Iceland (the Icelandic low) and the Azores (the Azores high) and just as El Niño, is an important factor in influencing the climate in the Pacific, the NAO influences the climate in Europe. A positive NAO phase is associated with anomalously low sea-level pressure in Iceland, strong meridional pressure gradients over the North Atlantic and intensified westerly winds. This corresponds to a strong inflow of cold air masses over the Alaska–Greenland region, warming air masses over the NW Atlantic Ocean, intensification of westerly winds reducing the cold Siberian air masses over NE Europe, and mild European winters. In contrast, a negative phase results in a reduced westerly airflow that migrates southwards. Simultaneously, the inflow of cold air masses from the Alaska–Greenland region is reduced whereas the inflow of cold Siberian air masses into eastern Europe is intensified, resulting in severe winters over Europe.

The NAO exhibits considerable interseasonal and inter-annual variability, and prolonged periods (several months) of both positive and negative phases of the pattern are common. Additionally, the wintertime NAO exhibits significant interannual and interdecadal variability. For example, the negative phase of the NAO dominated the circulation from the mid-1950s through the 1978/1979 winter. During this approximately 24 yr interval, there were 4 prominent periods of at least 3 yr, each in which the negative phase was dominant and the positive phase was notably absent. In fact, during the entire period the positive phase was observed in the seasonal mean only 3 times, and it never appeared in 2 consecutive years.

An abrupt transition to recurring positive phases of the NAO then occurred during the 1979/1980 winter, with the atmosphere remaining locked into this mode through the 1994/1995 winter season. During this 15 yr interval, a substantial negative phase of the pattern appeared only twice,

in the winters of 1984/1985 and 1985/1986. However, November 1995 to February 1996 was characterised by a return to the strong negative phase of the NAO. Halpert & Bell (1997, cited on NAO source webpage) recently documented the conditions accompanying this transition to the negative phase of the NAO. The 1996/1997 winter season has exhibited a more variable nature of the NAO, with negative phases of the pattern in December 1996 and January 1997 and positive phases in February and March 1997 (Fig. A1).

Clearly, the NAO does influence the climate strongly, for example Siegmund & Schrum (2001) linked the climate-induced variability in hydrographic and ecological processes with the wind and found an increase in wind speed of around 10%, which also coincided with an increase in the winter NAO index.

EA: East Atlantic teleconnection pattern index (September to April)

Source: ftp.ncep.noaa.gov/pub/cpc/wd52dg/data/indices/tele_index.nh

The East Atlantic (EA) pattern is the second of 3 prominent modes of low-frequency variability over the North Atlantic, appearing in all months except May to August. The pattern is structurally similar to that of the NAO, and consists of a N–S dipole of anomaly centres, which span the entire North Atlantic Ocean from east to west (Fig. A1). However, the anomaly centres in the EA are displaced SE to the approximate nodal lines of the NAO pattern. For this reason, the EA pattern is often mistaken as simply a slightly southward-shifted NAO pattern. In addition, the lower-latitude centre contains a strong subtropical link, reflecting large-scale modulations in the strength and location of the subtropical ridge. This subtropical link also makes the EA pattern distinct from its NAO counterpart.

EA–JET: East Atlantic jet pattern index (April to August)

Source: www.cpc.noaa.gov/data/teledoc/ea.html

The EA Jet pattern is the third primary mode of low-frequency variability found over the North Atlantic, appearing between April and August. This pattern also consists of a N–S dipole of anomaly centres, with 1 main centre located over the high latitudes of the eastern North Atlantic and Scandinavia, and the other located over Northern Africa and the Mediterranean Sea. A positive phase of the EA jet pattern reflects an intensification of westerly winds over the central latitudes of the eastern North Atlantic and over much of Europe, while a negative phase reflects a strong split-flow configuration over these regions, sometimes in association with long-lived blocking anticyclones in the vicinity of Greenland and Great Britain.

The time series of the EA jet pattern exhibits considerable interdecadal variability. For example, the 1971 to 1978 period was dominated by the negative phase of the pattern, while the 1985 to 1993 period was dominated by the positive phase of the pattern. In fact, from 1986 to 1993 the positive phase of the pattern was observed nearly 70% of the time (Fig. A1).

Appendix 2 (continued)

SCAN: Scandinavian teleconnection pattern, indices all months except June and July

Source: www.cpc.noaa.gov/data/teledoc/scand.html

The Scandinavian pattern consists of a primary circulation centre which spans Scandinavia and large portions of the Arctic Ocean north of Siberia. Two additional weaker centres with opposite sign to the Scandinavian centre are located over western Europe and over the Mongolia/western China sector. The Scandinavian pattern is a prominent mode of low frequency variability in all months except June and July, and has been previously referred to as the Eurasia-1 pattern. The positive phase of this pattern is associated with positive height anomalies, sometimes reflecting major blocking anticyclones, over Scandinavia and western Russia, while the negative phase of the pattern is associated with negative height anomalies over these regions. The time series for the Scandinavian pattern also exhibits relatively large interseasonal, interannual and interdecadal variability. For example, a negative phase of the pattern dominated the circulation from early 1964 through mid-1968 and from mid-1986 through early 1993. Negative phases of the pattern have also been prominent during winter 1988/1989, spring 1990, and winter/spring 1991/1992. In contrast, positive phases of the pattern were observed during much of 1972, 1976 and 1984 (Fig. A1).

Fig. A1 shows the time series of the standardised values of the atmospheric indices mentioned above.

Solar indices

The amount of energy that is radiated by the sun and reaches Earth depends on the distance between the sun and Earth and on the influence of refraction, absorption and scattering it encounters on its way. Because the distribution over Earth varies, it drives the motion of atmospheric and oceanic masses and so influences the global climate. The total solar radiation intensity has an approximately 11 yr cycle (Lean et al. 1995). The significance of the sun's cycles and the extent to which they influence the climate is still under debate (Nesme-Ribes et al. 1996). How much the sun contributes to global warming is also a controversial issue (Kristjánsson 2001). Lean et al. (1995) determined that before the industrial period, solar irradiance accounted for 86% of the global warming, for 50% since 1860, and for only 33% since 1970. Notwithstanding these controversies, it is clear that solar activity does influence the dynamics of the lower altitudes and therefore the amount of sunshine and cloud cover we experience (Mironova & Pudovkin 2002). As an indicator of solar activity we have 2 indices: the 'Solar Constant' time series and the 'International Sunspot Number' time series from 1700 to the present (Fig. A2).

SOLCON: Solar constant derived from solar irradiance with interpolated monthly values

Source: Lean et al. (1995), climexp.knmi.nl/selectyear.cgi

The solar constant is derived from solar irradiance (Lean et al. 1995) with interpolated monthly values by the Royal

Netherlands Institute of Meteorology (KNMI, G. J. van Oldenborgh). Winter and annual means were very similar; we used the annual mean. The solar constant is the power collected at the top of the atmosphere by a unit area perpendicular to the light path. Its designation is misleading since it is not a constant but varies latitudinally and seasonally.

SSN: Sunspot number

Source: Sunspot Index Data Centre (SIDC 2003), www.astro.oma.be/index.php3

The number of sunspots represents the magnitude of solar activity and has a cycle of approximately 11 yr, during which the number of sunspots differs between a maximum of a few tens to a few hundreds per month and a minimum of almost zero. There seems to be a strong link between the number of sunspots and the air temperature but this explains only the variation up to 1975. After this time, the observed and predicted temperatures diverged rapidly (Kristjánsson 2001). The winter and annual means were very similar; we used the annual mean (Fig. A2).

Climate indices

The KNMI monitors stations all over the Netherlands and we selected the station in De Kooy, in the north of Holland near the coast. We included wind data, temperature, precipitation, sunshine and air pressure. Initially we also had the same parameters for a coastal station in the south of the Netherlands (Vlissingen), but as these data series overlapped each other and would thus confuse the PCA, we omitted the Vlissingen data. Standardised time series are plotted in Fig. A3. Abbreviations used and description of the data series (all for De Kooy) are:

WINDIR: Prevailing wind direction in degrees ($360^\circ = N$, $270^\circ = W$, $180^\circ = S$, $90^\circ = E$)

WINSPE: Mean annual wind speed (0.1 m s^{-1})

AIRTEMP: Mean annual air temperature (0.1°C)

SUNSHI: Total annual sunshine duration (0.1 h)

PRECIP: Total annual precipitation amount (0.1 mm)

SAP: Mean annual surface air pressure (0.1 hPa)

CLOUD: Mean annual cloud cover (octants; 9 = sky invisible)

Log_SUMSTORM: No. of days in summer (Jun, Jul, Aug) with wind speed $>10.8 \text{ m s}^{-1}$ of >6 Beaufort

Source: www.knmi.nl/voorl/kd/lijsten/daggem/etmgeg_downl.cgi?language=nl

Because of outliers, data data was log-transformed prior to further analyses.

Other climate indices were:

Log_V_Ynsen: Total days with frost (i.e. minimum temperature $< 0^\circ\text{C}$) from November to March in De Bilt (station in

Appendix 2 (continued)

centre of the Netherlands), a location representative for the whole of the Netherlands.

Source: IJnsen (1988), with updated data from Mr. IJnsen
Because of outliers, the data was log-transformed prior to further analyses (Fig. A4).

WAVE_WIN: Mean wave height (m) at Buoy K13 in North Sea (winter average)

Source: www.golfklimaat.nl

Because this data set only started in 1979 it was omitted from the PCA and from the 1978/1979 regime shift analysis (Fig. A5).

WINSP_NS: Annual mean wind speed (m s^{-1}) over North Sea (Fig. A6)

Source: Siegismund & Schrum (2001), data used were taken from Fig. 2 of their article

Hydrographic/oceanographic indices

WADMHT: Annual mean high tide in the Wadden Sea (mm) above normal Amsterdam level (NAP)

Source: Dijkema (1997, with updates until 2002 from K. Dijkema)

The data are based on records of tidal gauges at 3 different locations in the province of Friesland in the north of the Netherlands. There seems to be an upward trend (2.9 mm yr^{-1} , after correction for wind effects and air pressure 2 mm yr^{-1}) but this is not significant according to Dijkema (1997) (Fig. A7).

ASTCE: Average surface air temperature ($^{\circ}\text{C}$) above central England (Fig. A8)

Source: Hadley Centre for Climate Prediction and Research (HCCPR 2002), www.defra.gov.uk/environment/statistics/des/index.htm

The average was calculated from the anomaly of surface air temperature from 1772 to 2001 compared to a 1961 to 1990 baseline.

WZTEMPWIN: Mean winter sea-surface temperature (December, January, February March) ($^{\circ}\text{C}$) at Marsdiep, western Wadden Sea (Fig. A9)

Source: H. van Aken, Netherlands Institute for Sea Research (unpubl.)

WZSAL: Mean annual sea surface salinity (ppt) at the tidal inlet Marsdiep, Wadden Sea

Source: H. van Aken, Netherlands Institute for Sea Research (unpubl.)

SAL_GB: Mean annual sea-surface salinity (ppt) of the German Bight and surroundings

Source: NW European Shelf Program (NOWESP) database available on www.ifm.uni-hamburg.de/outgoing/radach/nowesp/

Salinity was measured at the sea-surface. The salinity of the German Bight was very similar to the salinity of the (western) Wadden Sea. To prevent doubling of datasets and thus confusing PCA, we omitted the German Bight data series as the Wadden Sea data were more complete (Fig. A10).

SAL_NS: Annual average sea-surface salinity (ppt) in southern North Sea (International Council for the Exploration of the Sea [ICES] Quadrant IVb 50 to 55°N , 0 to 5°E)

Source: www.ices.dk/ocean/INDEX.HTM

ICES samples were taken by various cruises. Some of these were very close to shore and included sample locations in river mouths. Naturally the salinity in the estuaries and just offshore from major rivers will be very low and therefore influence the monthly/yearly mean. In order to reduce/eliminate these effects, we omitted these data points in the calculation of the annual means (Fig. A10).

SLP: Mean sea-level pressure in North Sea (0 to 6°E , 50 to 60°N)

Source: wesley.wwb.noaa.gov/ncep_data/index.html

As the available time series started in 1979, we omitted this variable from the PCA and from the 1978/1979 regime shift analysis (Fig. A11).

N/P_JFM: Winter average of the nitrate-phosphate relation (January, February, March) in southern North Sea (ICES Quadrant IVb 50 to 55°N , 0 to 5°E)

Source: www.ices.dk/ocean/INDEX.HTM

As for the North Sea salinity data, the nitrate and phosphate data, taken on the same ICES cruises, are influenced by the sample location. Rivers contain a much higher amount of these nutrients and we therefore omitted all data points close to river mouths (Fig. A12).

In the Internet and from the literature we were able to find various data sets regarding the sea-surface temperature ($^{\circ}\text{C}$) (SST) in the North Sea. Initially we gathered the SST from the southern North Sea (ICES), the northern North Sea (Reid et al. 2001a), the entire North Sea annually and seasonally (NOAA), the wider North Sea annually (BSH; Bundesamt für Seeschifffahrt und Hydrographie) and from the southern Norwegian coast and the German Bight (both NOAA data). When comparing the NOAA SST data set for the North Sea (50 to 60°N , 0 to 4°E) with the ICES SST (50 to 55°N , 0 to 5°E) and the BSH SST (51 to 62°N , 4°W to 12°E) the pattern was revealed to be very similar (Fig. A13).

Appendix 2 (continued)

The data from BSH comprised the largest North Sea area compared with the NOAA and ICES data. It was calculated from weekly SST grids (of 20 nautical miles or 1/3°) with the aim of obtaining an accurate insight into the spatio-temporal evolution (Loewe & Becker 2003). We therefore selected the BSH data series and calculated the first 9 yr by subtracting the average difference between the NOAA SST data and the BSH SST data to obtain an approximate value for the missing 1960 to 1968 years in the BSH data set. The data series from the German Bight and Norwegian coast were only available for January and only until 1994 and we therefore omitted them. As some biological processes are strongly linked with summer and others with winter temperatures we wanted to include seasonal averages as well. This left us the following 3 variables, which are shown in Fig. A14.

SST_NS: Annual average SST in North Sea (51 to 62° N, 4° W to 12° E; for accurate dimensions see web page of data source)

Source: www.bsh.de/aktdat/mk/M54ANOMe.html

SST_WIN: Mean winter SST in North Sea (50 to 60° N, 0 to 4° E), (January, February and March)

Source: iridl.ldeo.columbia.edu/SOURCES/.NOAA/.NCDC/.ERSST/.SST

SST_SUM: Mean summer SST in the North Sea (50 to 60° N, 0 to 4° E) (June, July and August)

Source: iridl.ldeo.columbia.edu/SOURCES/.NOAA/.NCDC/.ERSST/.SST

Biological indices

Prior to the data analysis, all biological time series were log-transformed to approximate linear distribution.

Vegetation

Data have been referenced to the area of 1980 (= 0); after this date, along the Friesland coastline, accretion has occurred in contrast to the Groninger coastline, where erosion has taken place. Along the coast of Friesland the marshland increased rapidly from 1975 until 1983, then slowly decreased, increasing again in the late 1980s. Along the coast of Groningen there was a slight increase from 1970 to 1975, then a rapid decrease that continued until the late 1980s, after which the marshland area very slowly increased again, although the net effect is still negative (i.e. a retreat inland from the dyke). Data before 1970 were not used as the marshland area was influenced by management techniques including the establishment of brushwood groynes, which decreased wave energy and currents and therefore increased sedimentation, leading to an increase in the marshland area. Data after this year are primarily influenced by the weather and therefore of interest to this study. Salt-marshes are subjected to tides

and annual variability in the mean high tide has an impact on the occurrence of plants in the salt-marsh zones which, in turn, protect the newly formed land from sedimentation (Fig. A15).

FRMARSH: Outer border marshland area along the coast of Friesland (m from dyke)

Source: Dijkema (1997)

GRMARSH: Outer border marshland area along the coast of Groningen (m from dyke)

Source: Dijkema (1997)

Marine micro- and macro-flora and fauna

Phytoplankton data from Cadée & Hegeman (2002) showed a sudden increase in the late 1970s with a doubling in values of chlorophyll *a*, primary production and phytoplankton biomass (Fig. A16). These high levels continued until the 1990s, suggesting that eutrophication was not the main reason for this increase as phosphate levels have diminished considerably since the successful cleaning of the river Rhine in the 1980s. In addition, the duration of *Phaeocystis* spp. blooms showed a sudden increase in the late 1970s and decreased after 1990 (Fig. A16). This increase was not related to eutrophication but seemed to be a natural phenomenon according to Cadée & Hegeman (2002). As a possible explanation for the decrease in Secchi disk visibility, the authors suggested the influence of the demersal fishery, whereby dredging leads to high turbidity levels (and therefore the derived suspended particulate matter [SPM] as calculated by C. J. Philippart [unpubl.], see below).

PHYTWIN: Annual winter (December to March) phytoplankton colour (colour unit) averaged for the North Sea, data-log transformed.

Source: Sir Alister Hardey Foundation for Ocean Science (SAHFOS) web page; Continuous Plankton Recorder (CPR) data: 192.171.163.165/data.htm

CHLOR_A: Annual average chlorophyll *a* concentration (m^{-3}), high-tide samples from the Marsdiep tidal inlet, western Wadden Sea

Source: Cadée & Hegeman (2002)

PRIMPROD: Phytoplankton primary production ($\text{gC m}^{-2} \text{yr}^{-1}$), high-tide samples from Marsdiep tidal inlet, western Wadden Sea

Source: Cadée & Hegeman (2002), data set taken from their Fig. 3

There were too many missing data points in the time series of the phytoplankton primary production and therefore it was omitted from the regime shift analysis.

Appendix 2 (continued)

SPM: Suspended particulate matter estimated from Secchi disk at high tide in Marsdiep (mean values for July, August and September)

Source: Turbidity data from (Cadée & Hegeman (2002), adapted to SPM by C. J. Philippart (unpubl.)

PHAEOBLO: Length of *Phaeocystis* spp. bloom periods (cells > 1000 cm⁻³) in days in Marsdiep inlet (western Wadden Sea)

Source: Cadée & Hegeman (2002), data series from their Fig. 4A

The zooplankton data were collected during the continuous plankton recorder (CPR) survey carried out by the Sir Alister Hardy Foundation for Ocean Science (SAHFOS). For details of the data collection methods and recording protocols we refer to their web site at: 192.171.163.165/cpr_survey.htm. Edwards et al. (2002) showed that there have been 2 large anomalous periods in the plankton data set corresponding with the years of our hypothesized regime shifts. They suggested a link with unusual ocean-climate conditions involving incursions of Atlantic water into the North Sea and reaching the southern continental North Sea in 1979, changing the regional temperatures and salinity and therefore the plankton composition. Unlike the data set of the Wadden Sea, phytoplankton and zooplankton abundance was significantly below average between the late 1970s and early 1980s. Similarly, the most abundant dinoflagellate (*Ceratium macroceros*) showed a steep population decline in the southern North Sea. The opposite occurred at the end of the 1980s, when warm Atlantic water came into the North Sea. However, these ocean-climate changes are not reflected very strongly in the zooplankton data sets in Fig. A17.

CALSUM: Abundance of total *Calanus* spp. for North Sea, summer averages (June to September), data log-transformed

Source: SAHFOS web page, CPR data. 192.171.163.165/data.htm

COPEP: Abundance of total copepods for North Sea, summer averages (June to September), data log-transformed

Source: SAHFOS web page, CPR data. 192.171.163.165/data.htm

CERMAC: Frequency of occurrence of dinoflagellate *Ceratium macroceros* in southern North Sea in CPR samples

Source: Edwards et al. (2002), data from their Fig. 3b

According to Beukema (1990), cold winters affect the macrozoobenthic community in a positive way, i.e. resulting in an increase in biomass. This was visible, with a lag-phase, after the cold winter of 1977/1978. In contrast, the warmer winters in the late 1980s resulted in a lower

biomass of macrozoobenthic species. Fig. A18 shows standardised time series of 6 different species.

POLYCHAET: Late winter polychaete biomass (mg ash-free dry weight m⁻²) in Balgzand, western Wadden Sea

Source: Beukema et al. (2002)

BIVALVE: Late winter bivalve biomass (mg ash-free dry weight m⁻²) in Balgzand, western Wadden Sea

Source: Beukema et al. (2002)

CAT_CEREDU: Catch of cockle *Cerastoderma edule* flesh (billion kg) in Dutch Wadden Sea

Source: J. Holstein, Federation of Cockle Fisheries (pers. comm.); data originally from Netherlands Institute for Fisheries Research (RIVO)

BIO_CEREDU: Biomass of cockle *Cerastoderma edule* flesh (billion kg) in Dutch Wadden Sea

Source: J. Holstein, Federation of Cockle Fisheries (pers. comm.); data originally from Ministry of Agriculture, Nature and Fisheries, 'Produktschap Vis' and the 'Producten' organization of the cockle fishery

GASTRO: Late winter gastropod biomass (mg ash-free dry weight m⁻²) in Balgzand, western Wadden Sea

Source: Beukema et al. (2002)

CRACRA: Mean ≥54 mm year class abundance of brown shrimp *Crangon crangon* on the west coast of Schleswig-Holstein, Germany

Source: Neudecker & Damm (1996), data their Fig. 1

Fishes

LANDXXX: International landing in 1000 t yr⁻¹ from ICES Quadrants III, IV, VII d

Source: Centre for Environment, Fisheries and Aquaculture Science (CEFAS), ICES. Digest of Environmental Statistics, published March 2002, www.defra.gov.uk/environment/statistics/des/-index.htm

These comprise the landing of cod (**LANDCOD**), herring (**sqrtLANDHER**), haddock (**LANDHAD**), whiting (**LANDWHIT**), sole (**LANDSOLE**) and plaice (**LANDPLAI**) (Fig. 19). Additionally, time series of the North Sea horse mackerel fishery yield is added.

HORSE: Catches of horse mackerel (1000 t yr⁻¹) in NE Atlantic

Source: Reid et al. (2001a)

Appendix 2 (continued)

The following 2 sets of data series obtained from the Netherlands Institute of Fisheries Research (RIVO) and shown in Figs. A20 & A21 were not taken into consideration for the PCA and only for the 1988/1989 regime shift analysis because of the late start of the data points.

NAMEFISH: Recruitment yield (avg no. h^{-1} fishing)

Source: Data from 'International Bottom Trawl Survey' carried out in North Sea by RIVO from 1978 to 2001. Final indices, 2002 preliminary values based on 390 hauls (data by courtesy of N. Daan and H. Heessen, RIVO)

Species comprise: Norway pout (**NOR_POU**), **SPRAT**, **COD**, and whiting (**WHIT**).

NAMEFISH (abbreviation of species name): Relative abundance of commercial and non-commercial fish species on Netherlands Continental Plateau (NCP) or in North Sea (including Skagerrak and Kattegat) calculated by N. Daan, RIVO.

Source: Daan (2000)

Along the Dutch coast these species comprise: *Osmerus eperlanus* (**OSMEPE**), *Limanda limanda* (**LIMLIM**), *Liparis liparis* (**LIPLIP**) and in the North Sea: *Clupea harengus* (**CLUHAR**), *Gadus morhua* (**GADMOH**), *Solea vulgaris* (**SOLVUL**), *Buglossidium luteum* (**BUGLUT**) (Fig. A21). Furthermore, RIVO supplied us with abundance data (ind. ha^{-1}) data on the NCP of 2 additional fish species, *Arnoglossus laterna* (**ARNLAT**) and *Echiichthys vipera* (**ECHVIP**) (Fig. A22).

Other time series of fish data was the catch data of recruits in Marsdiep tidal inlet, western Wadden Sea.

NAMEFISH (abbreviation of species name): Catch data of recruits (ind. d^{-1}) in Marsdiep tidal inlet

Source: Philippart et al. (1996, with updated data points from H. van der Veer, NIOZ)

These comprise: *Pleuronectes platessa* (**PLEPLA**), *Clupea harengus* (**CLUPHA**), *Alosa fallax* (**ALOFAL**), *Pollachius pollachius* (**POLPOL**) and *Merlangius merlangus* (**MERMER**) (Fig. A23)

Birds

Standardised time series of the following bird species are shown in Fig. A24.

OYSTERC: Total number of oystercatcher bird days in January for whole Dutch Wadden Sea

Source: Dutch centre for field ornithology (SOVON)

WORM.EAT: Total number of worm-eating waders bird days in January for the whole Dutch Wadden Sea, comprising: avocet, ringed plover, grey plover, dunlin, bar-tailed godwit

Source: Dutch centre for field ornithology (SOVON)

BRABRA: Number of dark-bellied Brent geese *Branta branta bernicla* in western Europe based on sightings and from 2000 to 2002 on estimation

Source: B. Ebbsing, Alterra-Wageningen (pers. comm.)

BRA_CHICK: Percentage of first year dark-bellied Brent geese chicks in western Europe (calculation based on sightings and survival rate)

Source: B. Ebbsing, Alterra-Wageningen (pers. comm.)

FLEDGE: Number of eider duck fledglings on Dutch Wadden Sea island of Vlieland

Source: Swennen (1991)

As data collection of the number of fledglings stopped in 1988 we did not include this time series in the PCA nor in the 1988 regime shift analysis.

Marine mammals

The population of seals is very dynamic: until 1960 hunting was the main reason for low numbers of seals in the entire Wadden Sea. In 1965 hunting was prohibited in the Netherlands, but due to the negative effects of pollution (especially the reduction of reproduction, which was prominent from the 1960s until the mid-1970s) the population was very slow to recover. From the mid-1970s to 1988 hunting was also prohibited in Germany and Denmark and the population increased. In 1988 a virus epidemic killed about 55 to 58% of the total population, and in the years after there still was selective death caused by the virus. From 1989 till 2002 the population grew explosively, as the negative effects of the pollution diminished to undetectable levels. In 2002 a new virus epidemic occurred, again killing about half the population (Reijnders 1981, Reijnders et al. 1997, Reijnders & Brasseur 2003). Along the North Sea coasts, seal species regularly strand on the beaches. The reason for the beach stranding is still unclear. In a literature review going as far back as 1800, S. Brasseur (Alterra-Texel) noted that there has been a strong increase in the number of seals washed ashore on the beaches of the Netherlands and Belgium since the 1980s, with a peak of 30 harp seals in 1987 (Fig. 25).

SEAL: Strandings of all seal species on the beaches of the southern North Sea

Source: S. Brasseur, Alterra-Texel (pers. comm.): data extracted from literature reviews

SEALPUPS: Percentage of counted pups in total number of sightings of the harbour seal *Phoca vitulina* in Dutch Wadden Sea

Source: Reijnders et al. (1997), Reijnders & Brasseur (2003)

PHOVIT: Population count of the harbour seal *Phoca vitulina* in Dutch Wadden Sea

Source: Reijnders et al. (1997), Reijnders (1981), with updates until 2002 from P. Reijnders, Alterra-Texel

PHOPHO: Total monthly average of sightings (h^{-1}) of harbour porpoise *Phocoena phocoena* from Dutch and Belgium North Sea coastline

Source: Marine mammal database: home.planet.nl/~camphuys/Cetacea.html

Appendix 2 (continued)

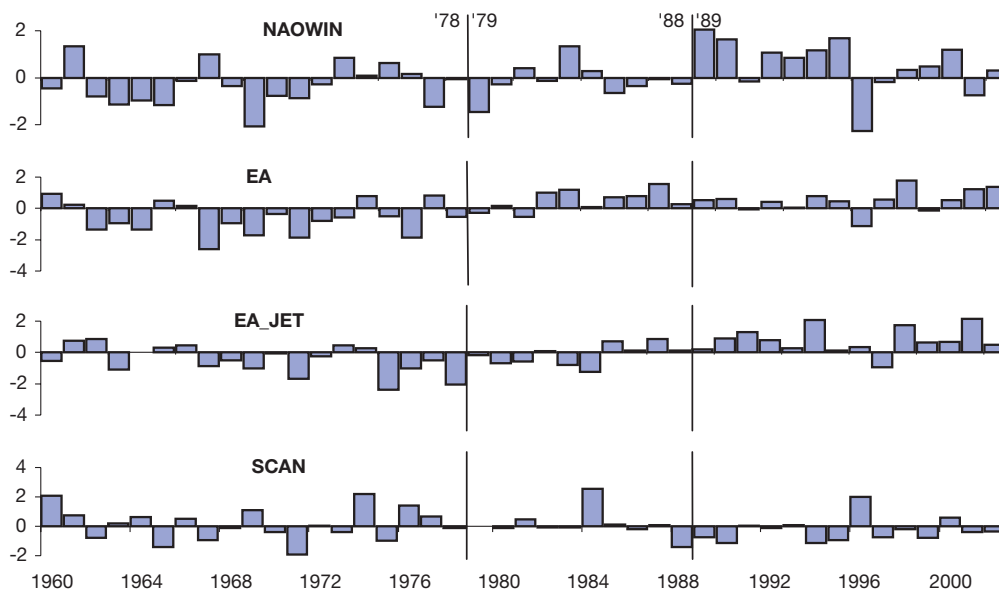


Fig. A1. Time series of 4 atmospheric indices, North Atlantic Oscillation Winter Index (NAOWIN), East Atlantic teleconnection pattern (EA), East Atlantic Jet pattern (EA_JET) and Scandinavian teleconnection pattern (SCAN). Data series standardised to zero mean +1 SD and plotted from 1960 to 2002

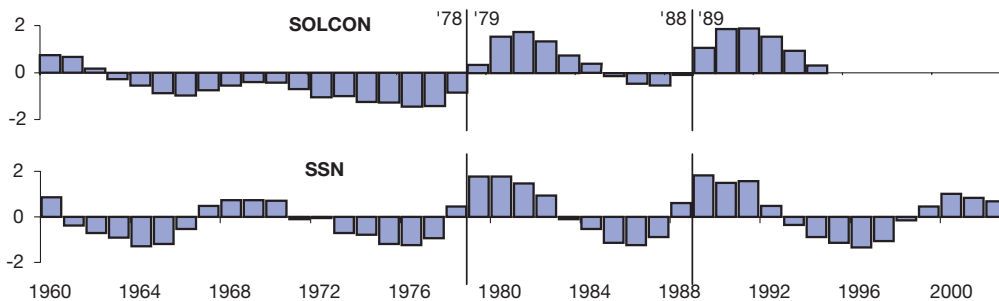


Fig. A2. Time series of solar constant (SOLCON) and number of sunspots (SSN). Data series standardised to zero mean +1 SD and plotted from 1960 to 2002 (for solar constant, data only available until 1994)

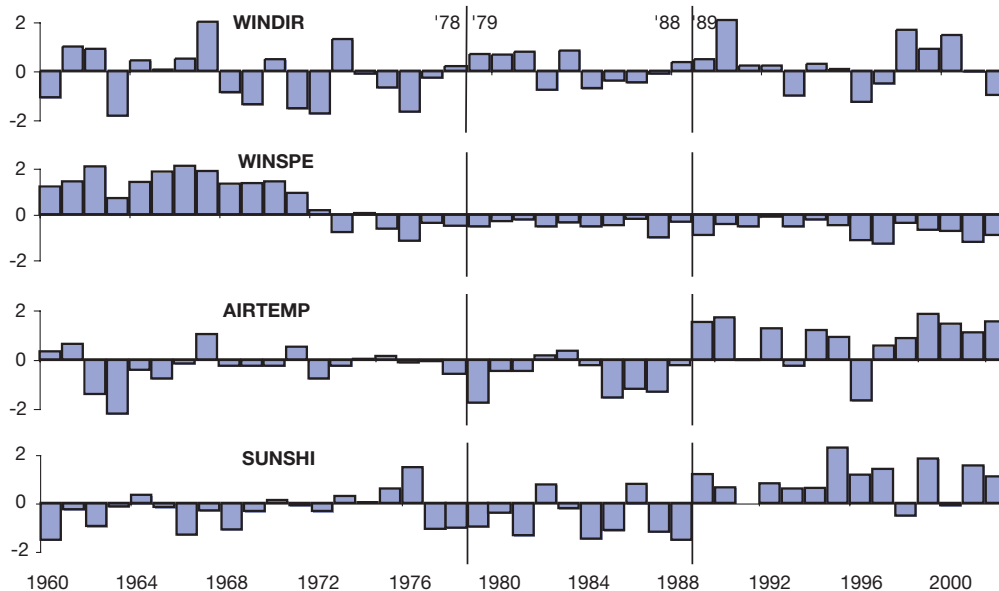


Fig. A3. (Above and following page)

Appendix 2 (continued)

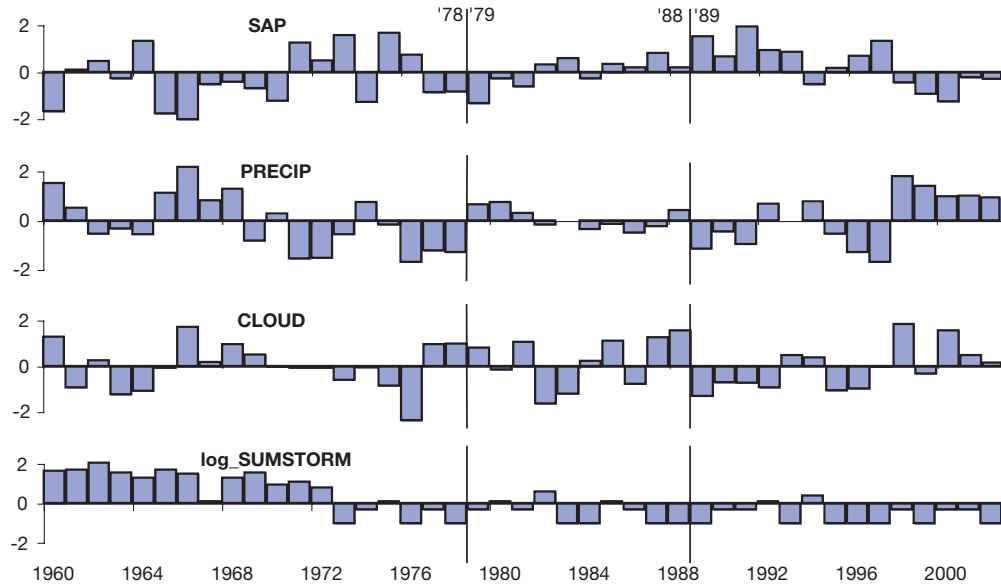


Fig. A3. (Above and previous page.) Time series of climate variables for De Kooy (North Holland): prevailing wind direction (WINDIR), mean annual wind speed (0.1 m s^{-1}) (WINSPE), mean annual air temperature (0.1°C) (AIRTEMP), total annual duration of sunshine (0.1 h) (SUNSHI), mean annual surface air pressure (0.1 hPa) (SAP), total annual precipitation (0.1 mm) (PRECIP), mean annual cloud cover (octants) (CLOUD) and log no. of summer storm days (log_SUMSTORM). Data series standardised to zero mean +1 SD and plotted from 1960 to 2002

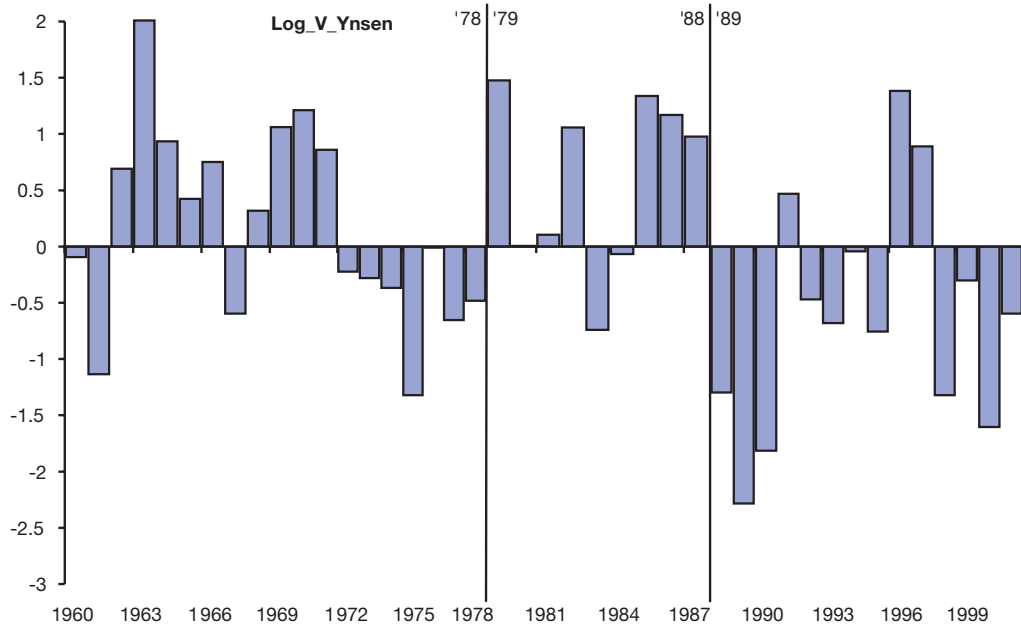


Fig. A4. Time series of numbers of days with frost (log_V_Ynsen) in the Netherlands. Data series standardised to zero mean +1 SD and plotted from 1960 to 2002

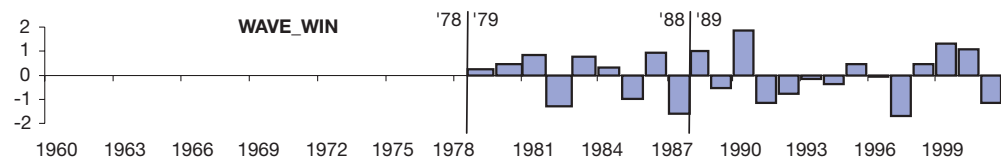


Fig. A5. Time series of mean winter wave height (m) (WAVE_WIN) in North Sea Buoy K13. Data series standardised to zero mean +1 SD and plotted from 1979 to 2001 (only data available)

Appendix 2 (continued)

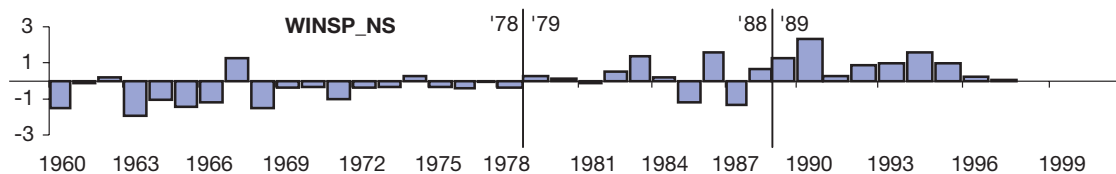


Fig. A6. Time series of annual mean wind speed (m s^{-1}) (WINSF_NS) over North Sea. Data series standardised to zero mean +1 SD and plotted from 1960 to 1997

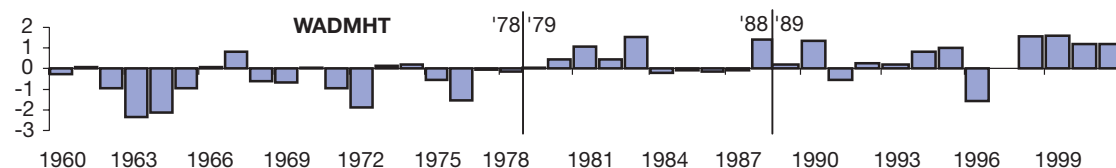


Fig. A7. Time series of the mean high tide in the Wadden Sea (mm) (WADMHT). Data series standardised to zero mean +1 SD and plotted from 1960 to 2001

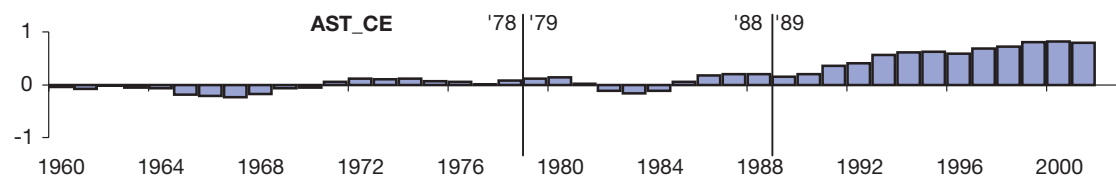


Fig. A8. Time series of anomaly of central England air temperature ($^{\circ}\text{C}$) (ASTCE) compared with 1961 to 1990 average. Data series standardised to zero mean +1 SD and plotted from 1960 to 2002

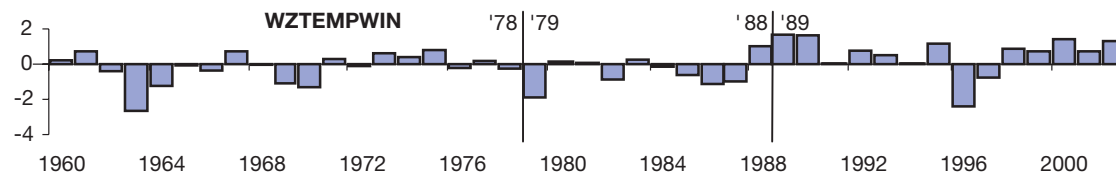


Fig. A9. Time series of winter sea-surface temperature ($^{\circ}\text{C}$) (WZTEMPWIN) in Dutch Wadden Sea. Data series standardised to zero mean +1 SD and plotted from 1960 to 2002

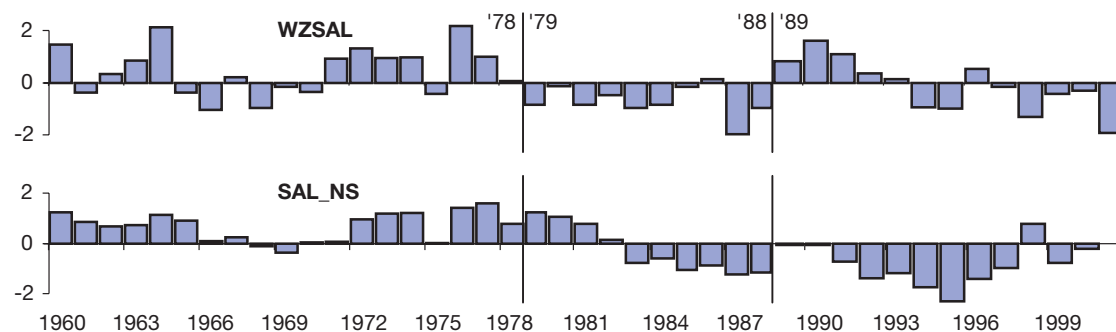


Fig. A10. Time series of surface salinity of Wadden Sea (pps-78) (WZSAL) and southern North Sea (50 to 55°N , 0 to 5°E) (SAL_NS). Data series standardised to zero mean +1 SD and plotted from 1960 to 2001

Appendix 2 (continued)

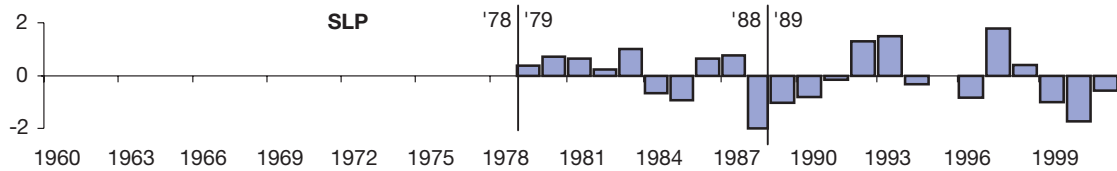


Fig. A11. Time series of average sea-level pressure (SLP) in North Sea. Data series standardised to zero mean +1 SD and plotted from 1979 to 2001

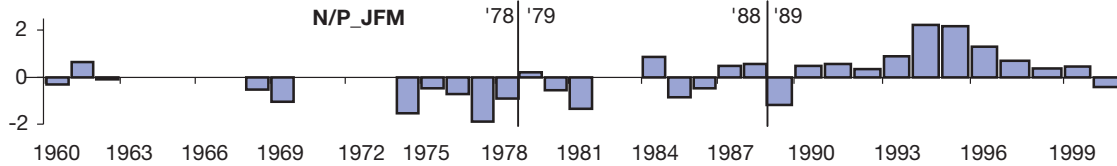


Fig. A12. Time series of nitrate:phosphate ratio in winter months (January to March) (NP_JFM). Data series standardised to zero mean +1 SD and plotted from 1960 to 2000 with some missing values

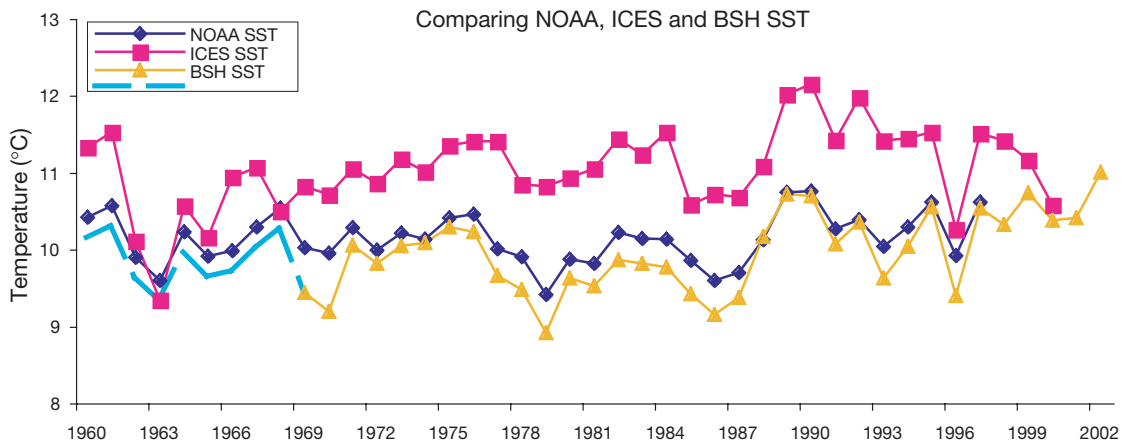


Fig. A13. Sea-surface temperature (SST) data series for North Sea from different sources: National Oceanographic and Atmospheric Organisation (NOAA), International Council for Exploration of the Sea (ICES), Bundesamt für Seeschifffahrt und Hydrographie (BSH). Light blue dashed line from 1960 to 1969 in BSH time series is calculated from NOAA data set

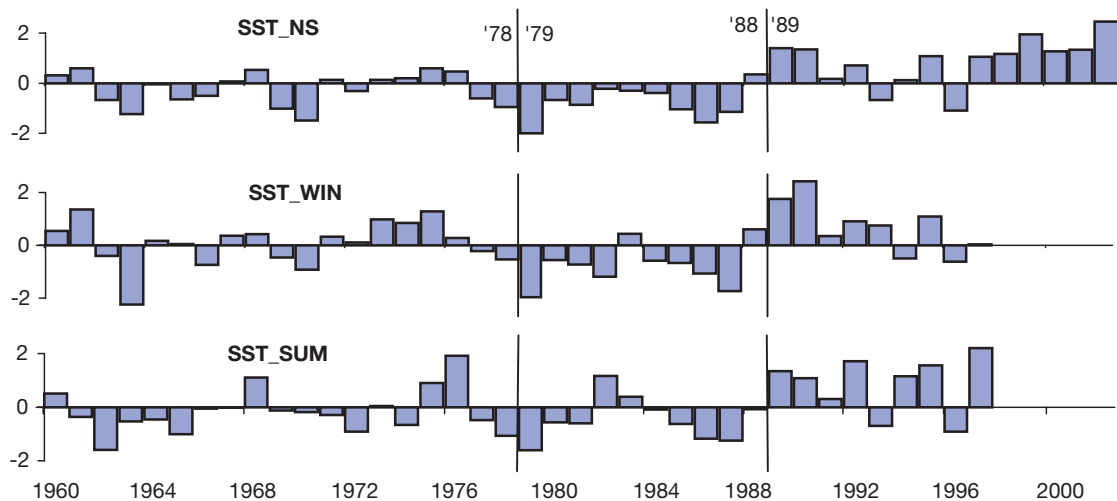


Fig. A14. Time series of annual mean sea-surface temperature for North Sea (SST_NS), annual average winter (from January to March) (SST_WIN) and summer SST (from June to July) (SST_SUM) of the North Sea. Data series standardised to zero mean +1 SD and plotted from 1960 to 2002 (SST_NS) and 1960 to 1997 (SST_WIN and SST_SUM)

Appendix 2 (continued)

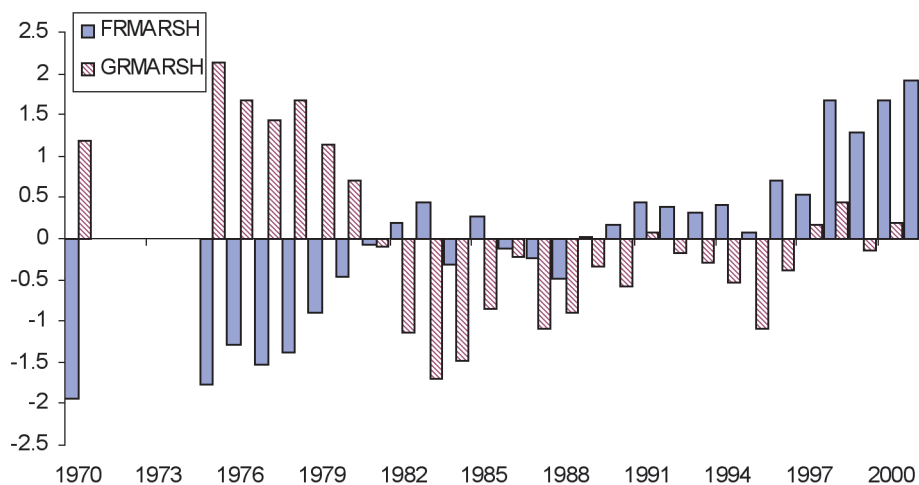


Fig. A15. Time series of marshland area (m from dyke) in 2 areas in NE Netherlands, Friesland (FRMARSH) and Groningen (GRMARSH). Data series standardised to zero mean +1 SD and plotted from 1960 to 2001

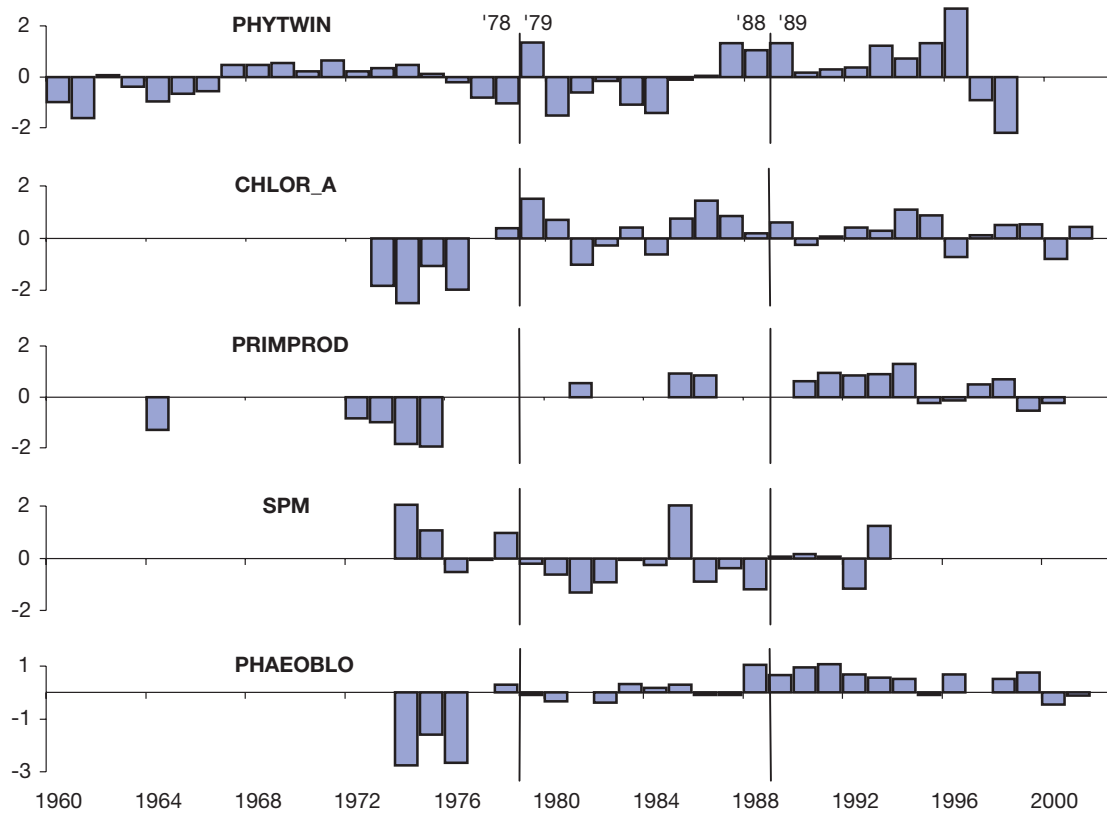


Fig. A16. Time series of phytoplankton characteristics: phytoplankton colour index in winter month (colour unit) for North Sea (PHYTWIN) and chlorophyll *a* concentration (m m^{-3}) (CHLOR_A), primary production ($\text{gC m}^{-2} \text{yr}^{-1}$) (PRIMPROD), suspended particulate matter (SPM) (recalculated from Secchi disk depth) and length of *Phaeocystis* sp. bloom (days) (PHAEOBLO), all in the Dutch Wadden Sea. All data series have been log-transformed and standardised to zero mean and 1 SD

Appendix 2 (continued)

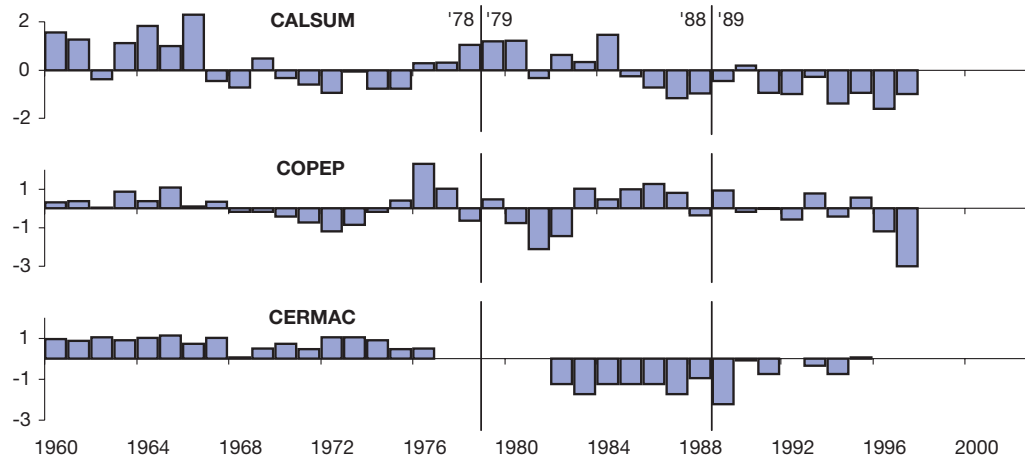


Fig. A17. Time series of zooplankton. Summer abundance of *Calanus* spp. (CALSUM), and total copepods (COPEP) and relative abundance of *Ceratum macroceros* (CERMAC) in continuous plankton recorder samples in North Sea. Data series log-transformed and standardised to zero mean +1 SD and plotted from 1960 to 1998

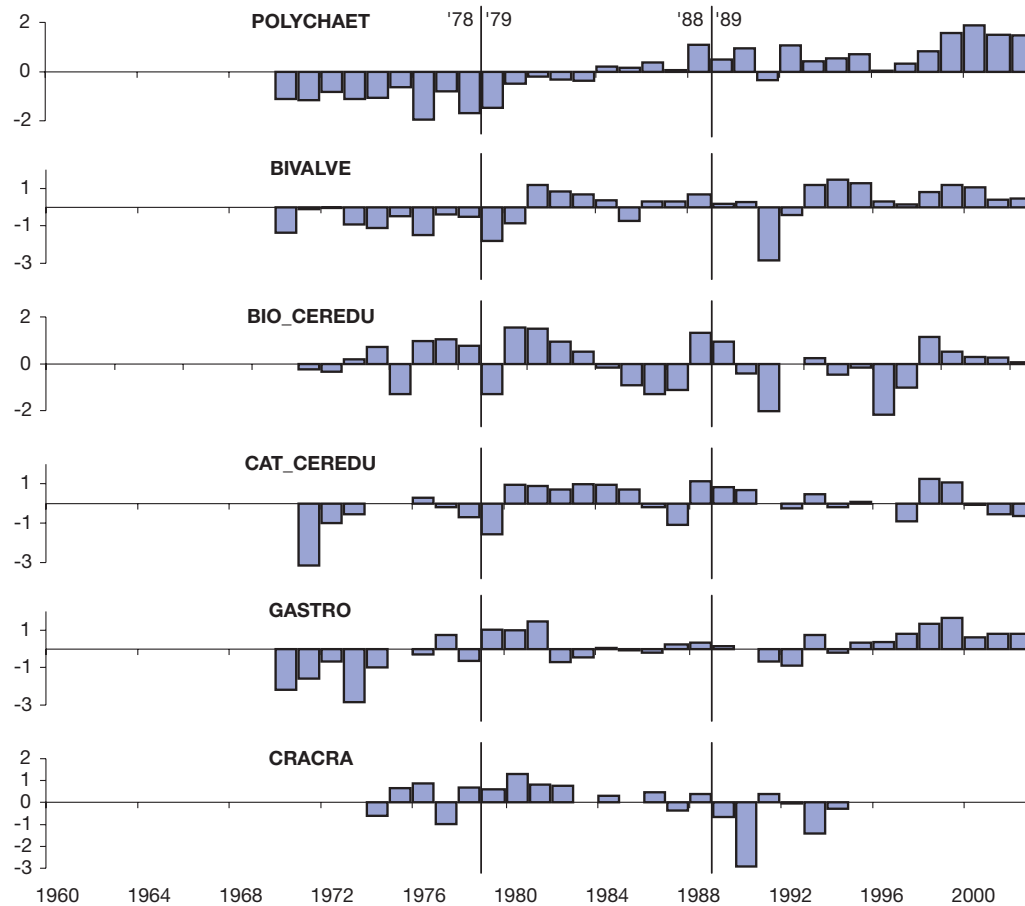
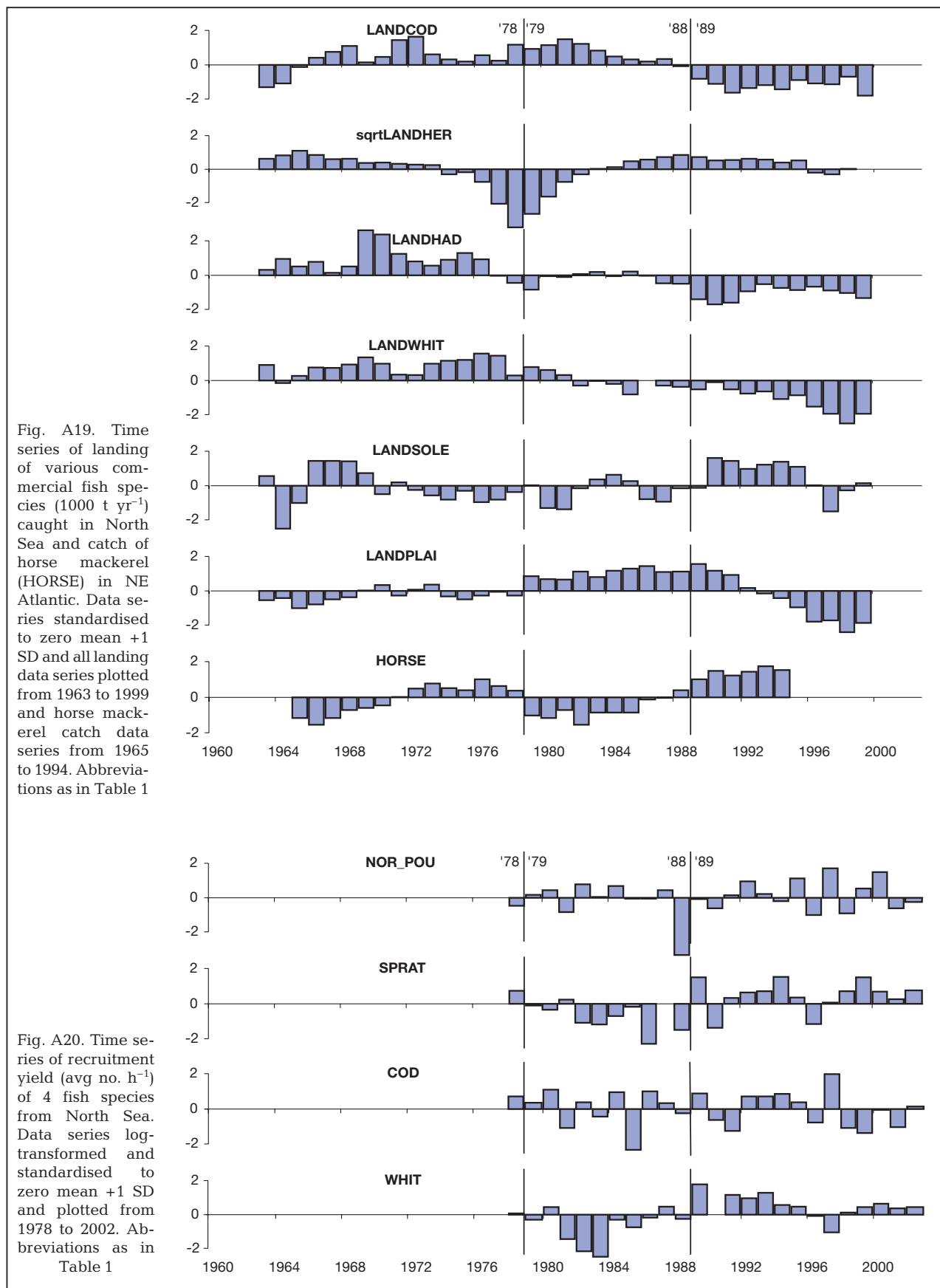


Fig. A18. Time series of macrobenthic organisms and brown shrimp *Crangon crangon*: abundance of polychaetes (POLYCHAET) and bivalves (BIVALVE) (mg AFDW m^{-2}) in Balgzand, western Wadden Sea, biomass and catch of cockles (billion kg) in Wadden Sea (BIO_CEREDU, CAT_CEREDU, respectively), abundance of gastropods (mg AFDW m^{-2}) in western Wadden Sea (GASTRO), and mean year class abundance of brown shrimp in northern part of German North Sea coast, Schleswig Holstein (CRACRA). All data series log-transformed and standardised to zero mean +1 SD and plotted from 1970 to 2002, brown shrimp data series plotted from 1974 to 1994

Appendix 2 (continued)



Appendix 2 (continued)

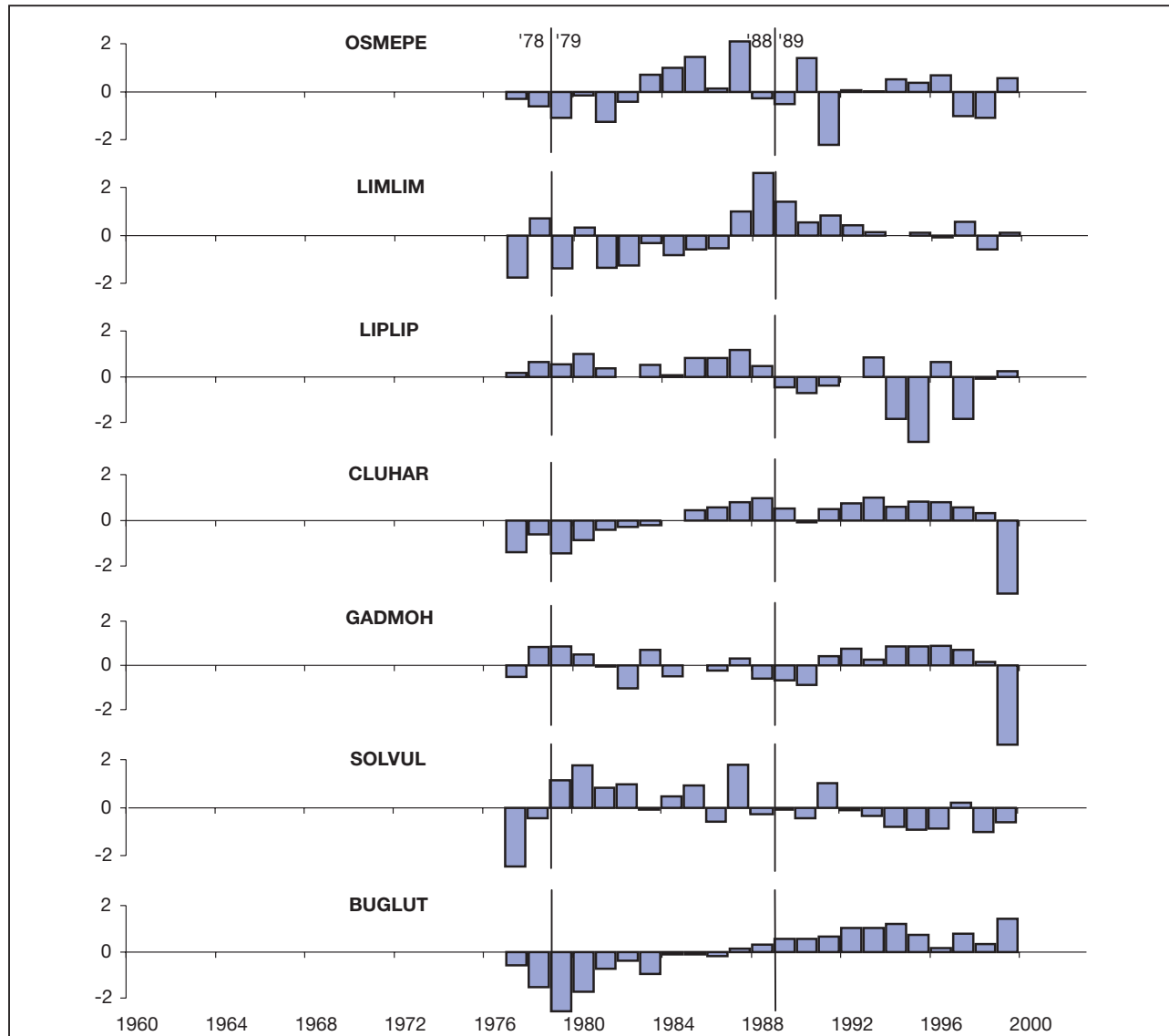


Fig. A21. Time series of relative abundance of commercial and non-commercial fish species on Netherlands continental plateau (NCP) and North Sea. Data series are log-transformed and standardised to zero mean +1 SD and plotted from 1977 to 1999. Abbreviations as in Table 1

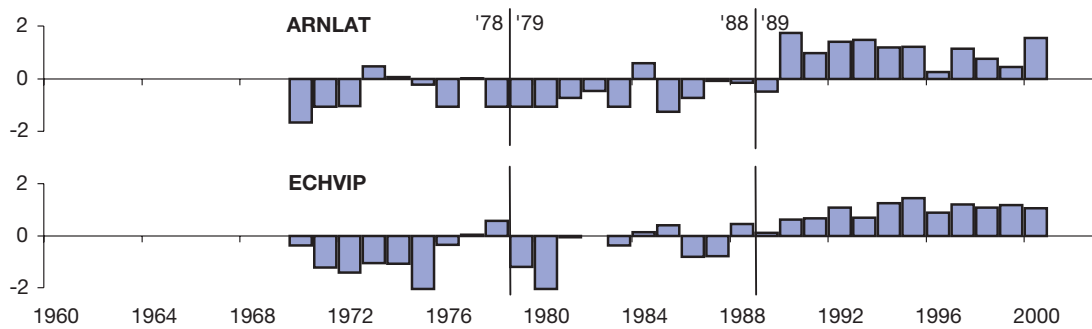


Fig. A22. Time series of abundance (no. ha⁻¹) of 2 non-commercial fish species on NCP, *Arnoglossus laterna* (ARNLAT) and *Echiichthys vipera* (ECHVIP). Data series log-transformed and standardised to zero mean +1 SD and plotted from 1970 to 2000

Appendix 2 (continued)

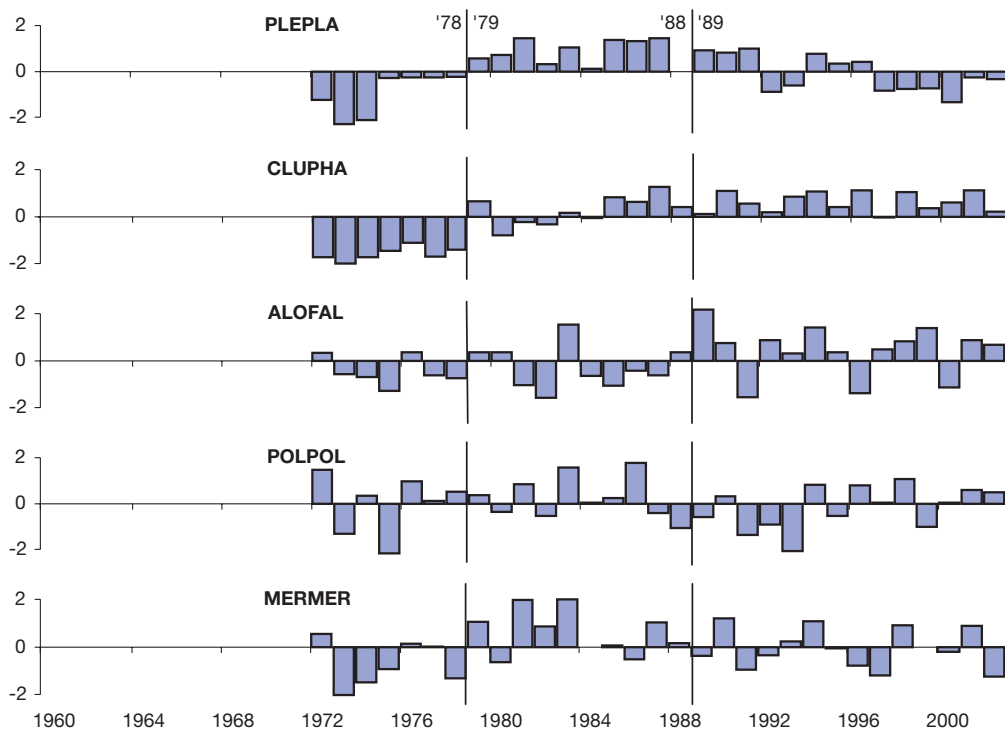


Fig. A23. Time series of recruitment yields (no. d^{-1}) of a random selection of 5 fish species caught in Marsdiep tidal inlet (western Wadden Sea). Data series log-transformed and standardised to zero mean +1 SD and plotted from 1972 to 2002. Abbreviations as in Table 1

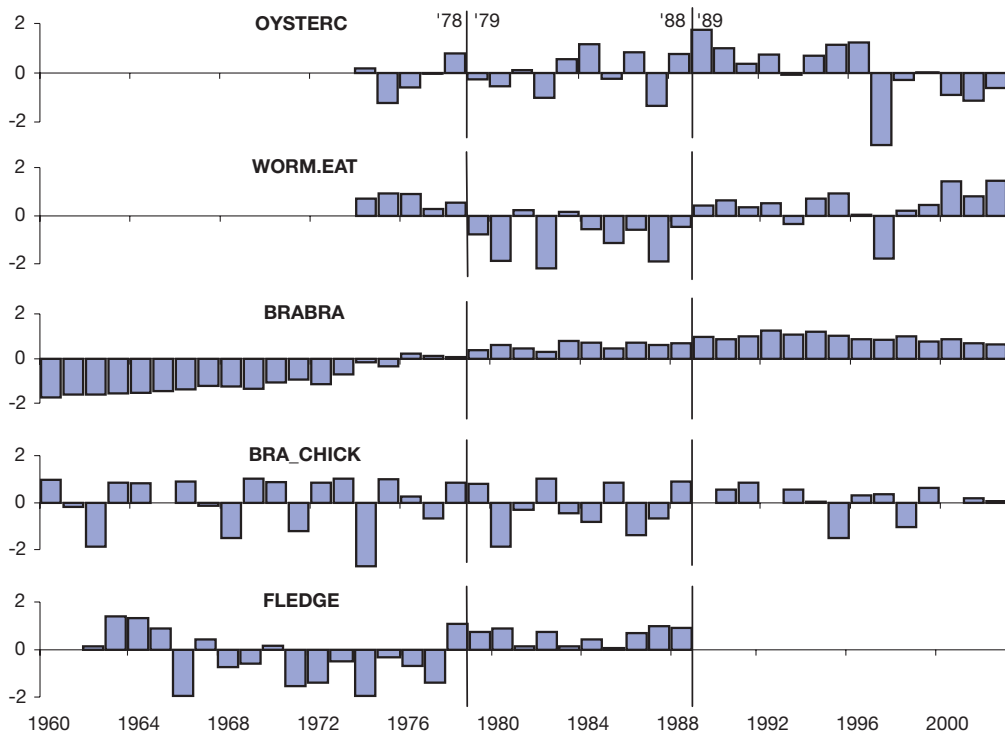


Fig. A24. Time series of abundance data of various bird species: no. bird days in January of oystercatchers (OYSTERC) and worm-eating waders (WORM-EAT) in Dutch Wadden Sea, no. dark-bellied Brent geese in western Europe (BRABRA), % first year Brent geese chicks (BRA_CHICK), and no. eider duck fledglings (FLEDGE) from Vlieland, Dutch Wadden Sea island. All data log-transformed and standardised to zero mean +1 SD

Appendix 2 (continued)

